Neuro-Oncology

Neuro-Oncology 16(12), 1585–1598, 2014
doi:10.1093/neuonc/nou128
Advance Access date 9 July 2014

Role of the endothelin axis in astrocyte- and endothelial cell-mediated chemoprotection of cancer cells

Seung Wook Kim, Hyun Jin Choi, Ho-Jeong Lee, Junqin He, Qiuyu Wu, Robert R. Langley, Isaiah J. Fidler, and Sun-Jin Kim

Department of Cancer Biology, Metastasis Research Laboratory, The University of Texas MD Anderson Cancer Center, Houston, Texas (S.W.K., H.J.C., H.-J.L., J.H., Q.W., R.R.L., I.J.F., S.-J.K.)

Corresponding Author: Isaiah J. Fidler, DVM, PhD, Department of Cancer Biology, Unit 173, The University of Texas MD Anderson Cancer Center, 1515 Holcombe Boulevard, Houston, TX 77030-4095 (ifidler@mdanderson.org).

See the editorial by Winkler, on pages 1565–1566.

Background. Recent evidence suggests that astrocytes protect cancer cells from chemotherapy by stimulating upregulation of anti-apoptotic genes in those cells. We investigated the possibility that activation of the endothelin axis orchestrates survival gene expression and chemoprotection in MDA-MB-231 breast cancer cells and H226 lung cancer cells.

Methods. Cancer cells, murine astrocytes, and murine fibroblasts were grown in isolation, and expression of endothelin (ET) peptides and ET receptors (ET_AR and ET_BR) compared with expression on cancer cells and astrocytes (or cancer cells and fibroblasts) that were co-incubated for 48 hours. Type-specific endothelin receptor antagonists were used to evaluate the contribution of ET_AR and ET_BR to astrocyte-induced activation of the protein kinase B (AKT)/mitogen-activated protein kinase (MAPK) signal transduction pathways, anti-apoptotic gene expression, and chemoprotection of cancer cells. We also investigated the chemoprotective potential of brain endothelial cells and microglial cells.

Results. Gap junction signaling between MDA-MB-231 cancer cells and astrocytes stimulates upregulation of interleukin 6 (IL-6) and IL-8 expression in cancer cells, which increases ET-1 production from astrocytes and ET receptor expression on cancer cells. ET-1 signals for activation of AKT/MAPK and upregulation of survival proteins that protect cancer cells from taxol. Brain endothelial cell-mediated chemoprotection of cancer cells also involves endothelin signaling. Dual antagonism of ET_AR and ET_BR is required to abolish astrocyte- and endothelial cell-mediated chemoprotection.

Conclusions. Bidirectional signaling between astrocytes and cancer cells involves upregulation and activation of the endothelin axis, which protects cancer cells from cytotoxicity induced by chemotherapeutic drugs.

Keywords: astrocytes, brain metastasis, breast cancer, endothelin, therapeutic resistance.

Approximately 200 000 cases of brain metastases occur in the United States each year.[1] Brain metastasis is associated with poor prognosis, neurological deterioration, diminished quality of life, and extremely short survival.[2] Indeed, the median survival time for untreated patients is 1–2 months[3] and improves to only 4–6 months for patients treated with chemotherapy and conventional radiotherapy.[4] The limited response of brain metastases to chemotherapy has been attributed to structural (ie, tight junctions) and functional (eg, P-glycoprotein) properties of the blood-brain barrier that prevent cytotoxic drugs from entering into the central nervous system (CNS).[5,6] However, experimental studies have shown that the blood-brain barrier is breached once metastases exceed 0.2 mm in diameter,[7,8] suggesting that additional mechanisms may contribute to the chemoresistant phenotype of brain metastases. An increased understanding of the mechanisms that mediate therapeutic resistance of brain metastases is critical for developing new treatment strategies that improve clinical outcomes.

Reactive astrogliosis is widely regarded as the most important histopathological indicator of diseased CNS tissue, regardless of etiology.[9] Reactive astrocytes encircle and infiltrate cancer cells residing in the brain.[10,11] Recently, we patterned reactive astrogliosis in vitro by co-incubating melanoma cells with astrocytes and discovered that gap junction-mediated communication protected melanoma cells from chemotherapeutic agents.[12] A more intensive examination, which employed cross-species hybridization of microarrays on human cancer cells that were co-incubated with murine astrocytes, revealed that direct contact between astrocytes and cancer cells leads to marked alterations in the cancer cell transcriptome including upregulation of the survival-related

Received 16 December 2013; accepted 10 June 2014

genes, glutathione S transferase alpha 5 (*GSTA5*), BCL2-like 1 (*BCL2L1*), and TWIST-related protein 1 (*TWIST1*).[13] Functional studies demonstrated a role for this subset of genes in protecting cancer cells from chemotherapy, and the gene products were localized to cancer cells in clinical cases of brain metastases.[13] However, the astrocyte signal that stimulates survival gene expression in cancer cells remained unknown.

Several lines of evidence have suggested a potential role for the small (21-amino acid) endothelin peptides in mediating anti-apoptotic gene expression and chemoprotection in cancer cells. The endothelin signaling pathway includes 3 peptides (ET-1, ET-2, and ET-3), which mediate their activity by binding to 2 high-affinity G-protein–coupled receptors, ET_AR and ET_BR.[14] Immunohistochemical analysis of a large series of human brain metastasis cases revealed that peritumoral astrocytes overexpress endothelin in 85% of metastases.[15] Reactive astrocytes are also reported to overexpress endothelin in several other CNS pathologies.[16] A comparison of gene expression profiles between melanoma cell variants, which spontaneously metastasized to the brain and parental cells with low metastatic potential, led to the identification of ET_BR as a critical determinant in the stepwise progression of melanoma to the brain metastatic phenotype.[17] ET-1 has also been shown to signal for activation of survival programs in several types of cancer cells.[18–20]

The above-mentioned studies prompted us to hypothesize that endothelin-mediated signaling between cancer cells and astrocytes and/or endothelial cells leads to the upregulation of survival genes in cancer cells and thus protection from chemotherapy. Herein, we examined how astrocytes and endothelial cells interact with MDA-MB-231 breast cancer cells and H226 non–small cell lung cancer (NSCLC) cells to modulate different components of the endothelin signaling axis and describe the impact on cancer cell survival.

Materials and Methods

Reagents

The following antibodies were used in this study: anti-ET_AR (BD Biosciences); anti-ET_BR (Santa Cruz Biotechnology); anti-glutathione *S*-transferase A5 (GSTA5) (Novus Biologicals); anti-phospho-serine, anti-IL-6 (AbCam); anti-IL-8 (Invitrogen); anti-AKT, anti-phospho-AKT (Ser-473), anti-MAPK, anti-phospho-MAPK (Thr-202 and Tyr-204), anti-TWIST1 and anti-BCL2L1 (Cell Signaling Technology); anti-β-actin (AC-15) (Sigma-Aldrich); and rabbit anti-mouse Alexa 647 antibody and goat anti-mouse Alexa 488 antibody (Molecular Probes).

The selective ET_AR antagonist BQ123, selective ET_BR antagonist BQ788, and endothelin-1 were from Sigma-Aldrich. Taxol was purchased from Bristol-Myers Squibb, and macitentan (ACT-064992) was provided by Actelion Pharmaceuticals, Ltd.[21] Calcein AM and DiI cell labeling dyes were purchased from Molecular Probes. Carbenoxolone (CBX), a gap-junction inhibitor,[12] was purchased from Sigma-Aldrich. Human recombinant IL-6 and IL-8 were purchased from R&D Systems.

Cell Lines

Human MDA-MB-231 breast cancer cells,[13] human H226 NSCLC cancer cells,[22] and murine NIH 3T3 fibroblasts[13] were maintained in complete Eagle's minimum essential medium (MEM) supplemented with 10% fetal bovine serum (FBS) (HyClone). The immortalized murine C8-B4 microglial cell line was a gift from Dr. D. Trisler (University of Maryland), and human astrocytes were purchased from ScienCell Research Laboratories. Murine astrocytes[23] and brain endothelial cells[24] were established in our laboratory and have been described previously. Cell lines were tested at the MD Anderson Characterized Cell Line Core Facility using short-tandem repeats DNA profiling. Astrocytes, fibroblasts, endothelial cells, and microglial cells were transfected with green fluorescence protein (GFP) genes as previously described.[25]

Immunofluorescence Analysis

MDA-MB-231 cells were plated onto 4-well chamber slides (Cole-Parmer) at a density of 5×10^4 cells/well in MEM containing 10% FBS. The slides were placed in a 37°C incubator for 24 hours and then incubated for 12 hours in MEM containing 0.1% FBS or treated for 30 minutes with 100 nM of ET-1. The cells were fixed in a methanol-acetone solution (1:1, vol/vol), incubated in blocking solution (4% fish gel) (Sigma-Aldrich) for 20 minutes, and then incubated at 4°C overnight with primary antibodies (1:100). Control samples were incubated with corresponding IgG isotype antibodies (1:100). Samples were rinsed and then incubated with goat anti-rabbit Alexa 647 antibody (1:600) for 1 hour. Slides were rinsed before incubating with 4′-6-diamidino-2-phenylindoe (DAPI) (Life Technologies) for 5 minutes to label the cell nuclei. Samples were visualized with a BX-51 microscope equipped with a DP71 digital camera, and the images were processed using DP Manager software (Olympus).

Chemoprotection Assay

To evaluate the effect of astrocytes, fibroblasts, brain-derived endothelial cells, and microglial cells on the sensitivity of cancer cells to chemotherapeutic agents, we performed an in vitro chemoprotection assay as described previously.[13] In brief, astrocytes, endothelial cells, microglial cells, and 3T3 fibroblasts were transfected with GFP and plated along with MDA-MB-231 breast cancer cells or NCI-H226 NSCLC cells (cancer cell:test cell plating ratio of 1:2 was used in all co-culture studies) and allowed to stabilize overnight. The media were replaced with fresh MEM containing 15 ng/mL of taxol. After 48 hours, the GFP-labeled cells were separated from cancer cells by fluorescence-activated cell sorting (FACS), and the apoptotic index of cancer cells was determined by FACS analysis of propidium iodide-stained DNA as described previously.[13]

To determine whether astrocyte-mediated protection of cancer cells was due to activation of the endothelin signaling pathway, we pre-incubated the cancer cells with the endothelin receptor antagonists (BQ123, BQ788, or macitentan) or ET-1 peptides for 2 hours and then co-incubated the cells with astrocytes (or control fibroblasts) in the presence or absence of 15 ng/mL of taxol. The effect of taxol on cancer cells co-incubated with brain endothelial cells and microglial cells was also studied. To determine if direct contact was necessary for induction of anti-apoptotic genes in cancer cells, we separated individual cell types by a 0.4-μm membrane in transwell chambers (Costar). Upper inserts containing 1×10^5 cancer cells were placed over 2×10^5 astrocytes that were seeded on lower chambers, and

the cells were co-incubated for 48 hours in Dulbecco's modified Eagle's medium (DMEM) containing 10% FBS. The potential role of astrocyte-derived soluble factors in modulating expression of survival genes and proteins was assessed using astrocyte-conditioned media, which was generated by plating astrocytes onto 6-well plates at a density of 0.5×10^6/well in 2 mL of DMEM supplemented with 10% FBS for 48 hours. In other experiments, cancer cells were pretreated for 2 hours with 100 μM CBX prior to co-incubating with astrocytes (or other cell type) to study the role of gap junction communication in chemoprotection. In all cases, the apoptotic index of cancer cells was determined 48 hours later by measuring propidium iodide labeling, and the results were expressed as means ± standard deviation (SD) from experiments conducted in triplicate.

Real-time Polymerase Chain Reaction Analysis

Total RNA was extracted from the cells using the Qiagen RNeasy mini kit (Qiagen). First-strand cDNA was synthesized from 5 μg RNA using SuperScript III reverse transcriptase (Life Technologies). Real-time (RT-) PCR was performed using TaqMan Universal PCR MasterMix and quantified with an ABI 7500 RT-PCR system (Applied Biosystems). The following TaqMan gene expression assays were used in our study: human *ET_AR* (Hs00609865_m1); human *ET_BR* (Hs00240747_m1); human *BCL2L1* (Hs00169141_m1); human *GSTA5* (Hs00604085_m1); human *TWIST1* (Hs00361186); human *ET-1* (Hs00174961_m1); human *ET-2* (Hs00171177_m1); human *ET-3* (Hs01012714_m1); human *IL-6* (Hs00985639_m1); human *IL-8* (Hs00174103_m1); mouse *ET-1* (Mm00438656_m1); mouse *ET-2* (Mm00432983_m1); and mouse *ET-3* (Mm00432986_m1) (all from Applied Biosystems). The 18S rRNA was used as an endogenous control, and relative mRNA expression was calculated using the $\Delta\Delta Ct$ method.[26] Results are expressed as means ± SD of mRNA relative to that of control.

Western Blot Analysis

For co-culture experiments, a total of 2×10^6 cells (cancer cells plus astrocytes or 3T3 fibroblasts) were plated onto 100 mm culture dishes and co-incubated for 24 hours. Cancer cells were isolated by FACS, washed twice with PBS, and lysed with buffer. To determine the effects of ET-1 stimulation on cancer cell proteins, the cells were plated onto 6-well plates at a density of 0.5×10^6 cells/well in MEM supplemented with 0.1% FBS. After a 24-hour period, the media were aspirated and replaced with ET-1 peptides for dose- and time-related studies. We used identical conditions when analyzing the effects of IL-6 and IL-8 on astrocytes or cancer cells. Next, 50 μg of total protein was separated by electrophoresis on 4–12% Nu-PAGE gels (Life Technologies) and transferred to nitrocellulose membranes. Membranes were blocked for 1 hour and incubated overnight at 4°C with primary antibodies (1:1000). The membranes were rinsed, incubated with horseradish peroxidase-conjugated secondary antibodies (1:3000), and visualized by enhanced chemiluminescence (Amersham).

Co-immunoprecipitation Analysis

A total of 3×10^6 cells (cancer cells only or cancer cells plus astrocytes or fibroblasts) were incubated on 100 mm culture dishes for 6 hours. In some experiments, cancer cells were stimulated with ET-1. In co-culture experiments, the cancer cells were separated from GFP-labeled astrocytes or fibroblasts and lysed in buffer. Then, 500 μg of whole-cell lysates were precleared with protein A agarose beads (Santa Cruz Biotechnology) for 2 hours at 4°C and incubated with the following antibodies: 2 μg of mouse or rabbit IgG (Santa Cruz Biotechnology), 2 μg of mouse monoclonal ET_AR antibody, or 2 μg of a rabbit polyclonal ET_BR antibody. After an overnight incubation at 4°C, the protein complexes were pulled down using protein-A agarose beads (4 h at 4°C). The beads were washed twice, pelleted by gentle centrifugation, resuspended in 20 μL of 2X Laemmli SDS sample buffer, separated by 4%–12% Nu-PAGE gel electrophoresis, and the proteins were transferred to nitrocellulose membranes. To determine whether endothelin receptors were phosphorylated, membranes were incubated with a phosphoserine antibody followed by incubation with horseradish peroxidase-conjugated secondary antibodies (1:3000). Horseradish peroxidase (HRP) activity was detected using enhanced chemoluminescence.

RNA Interference

RNA interference was performed on the MDA-MB-231 cancer cells using Lipofectamine 2000 (Life Technologies) according to the manufacturer's instructions. For silencing target proteins, siRNAs specific for ET_AR, ET_BR, IL-6, IL-8, and nontargeting control siRNAs were purchased from Santa Cruz Biotechnology. The siRNA sequences for ET_AR and ET_BR were 5′- GCAACCUUCUGCAUUCAUAtt-3′ and 5′-CAACAUGGCUUCACUGAAUtt-3′, respectively. The siRNA sequence for IL-6 and IL-8 were 5′-CAGAACGAAUUGACAACAtt-3′ and 5′-GGGUGCAGAGGGUUGUGGAGATT-3′, respectively. Cells were transfected with 100 nM siRNAs when they were 50% confluent, and knockdown of target proteins was confirmed by PCR or Western blot analysis.

Enzyme-linked Immunosorbent Assay for ET-1, IL-6, and IL-8 Expression

ET-1 protein produced by murine astrocytes, murine fibroblasts, and co-cultures containing human cancer cells with astrocytes or fibroblasts was measured using a standard ELISA kit measuring ET-1 (R&D Systems) according to the manufacturer's instructions. IL-6 and IL-8 were measured using ELISA kits purchased from Thermo Fisher Scientific. For co-culture experiments, we plated a total of 0.5×10^5 cells/well onto 6-well plates in DMEM with 10% FBS for 48 hours. In other studies, 2.0×10^5 astrocytes were stimulated with 100 ng/mL of IL-6 or IL-8 for 24 hours before collecting supernatants. The assays were conducted in triplicate, and the absorbance of the samples was compared with the standard curve.

Cell Cycle Analysis

To determine whether co-incubation of cancer cells with astrocytes altered the cell cycle distribution of cancer cells, we plated cancer cells alone or with astrocytes onto 6-well plates at a total density of 2.0×10^5 cells/well in MEM containing 10% FBS. The following day, the media were replaced, and the cells were incubated for 48 hours. Cancer cells were collected, washed, and fixed in 75% ethanol for 1 hour and then stained with 25 μg/mL

propidium idodide containing 0.1 U/mL RNAse. The DNA content of cells was analyzed with FACS.

Evaluation of Gap Junctional Communication

We evaluated the gap junctional communication between MDA-MB-231 cancer cells and astrocytes or brain endothelial cells using a dye transfer assay as previously described.[12] In brief, astrocytes and endothelial cells (donor cells) were labeled with calcein-AM (5 μM) for 30 minutes, and cancer cells (recipient cells) were labeled with DiI (5 μM) for 30 minutes (both at 37°C). Cells were rinsed several times and then co-incubated in 6-well plates for 6 hours. Next, the cells were harvested and analyzed by FACS to determine the fraction of DiI-positive cancer cells containing calcein. In some experiments, DiI-positive cancer cells were pre-incubated with 100 μM of CBX for 2 hours before co-incubation with donor cells. In other studies, the individually labeled cell types were separated by a 0.4-μm membrane in transwell chambers using the plating conditions described above and evaluated after 6 hours.

Data Analysis

Statistical analysis was performed with the Prism program (GraphPad Software, version 6.01) using the Student's *t* test. $P < .05$ was considered statistically significant.

Results

MDA-MB-231 Cancer Cell-astrocyte Interaction Leads to Upregulation and Activation of the Endothelin Axis

First, we measured constitutive gene expression of ET-1, ET-2, and ET-3 by murine astrocytes, murine fibroblasts, and MDA-MB-231 cells to determine whether gene expression levels were modulated when the cancer cells were co-incubated for 48 hours with astrocytes (or fibroblasts). Murine ET-1 gene expression increased 5-fold when astrocytes were co-incubated with MDA-MB-231 cancer cells (Fig. 1A), which was confirmed by ELISA (Supplementary Fig. S1). Co-culture of astrocytes with cancer cells had no effect on murine ET-2 mRNA expression or human ET-1 or ET-2 mRNA expression (Fig. 1A; Supplementary Figures S2A and S2B). No cell type expressed the ET-3 isoform. The level of murine ET-1 or ET-2 mRNA expression was not significantly increased in fibroblasts cultured alone or with cancer cells (data not shown). When mouse primers were used, no PCR products were detected in PCR-amplified human MDA-MB-231 cells, and no PCR products were observed in PCR-amplified murine cells when human primers were used.

We next measured ET_AR and ET_BR expression in MDA-MB-231 cells cultured alone or with murine astrocytes or fibroblasts. The schematic cartoon in Fig. 1B shows the overall experimental design. ET_AR and ET_BR gene expression was significantly increased in cancer cells that were cultured with astrocytes when compared with cancer cells cultured alone (2.5 ± 0.78-fold; $P < .05$ and 1.87 ± 0.5-fold; $P < .05$, respectively) (Fig. 1C). These results were confirmed by Western blot analysis (Fig. 1D). Co-incubating MDA-MB-231 cells with fibroblasts had no effect on cancer cell expression of ET_AR or ET_BR. Co-immunoprecipitation analysis of MDA-MB-231 cancer cells cultured alone or with GFP-labeled murine astrocytes indicated that murine astrocytes, but not fibroblasts, stimulated phosphorylation of ET_AR and ET_BR (Fig. 1E). This finding was confirmed by immunofluorescence microscopy (Supplementary Figs. S3A and S3B).

To determine if astrocyte-induced modulation of the endothelin axis was unique to MDA-MB-231 cancer cells, we examined astrocyte interactions with H226 NSCLC cells. ET-1 gene expression increased 7-fold in astrocytes that were co-incubated with H226 cells (Supplemental Fig. S4A), which was confirmed by ELISA (Supplemental Fig. S4B). We also noted that ET_AR and ET_BR were upregulated in H226 cells co-incubated with astrocytes (Supplemental Fig. S4C), and the receptors were phosphorylated (Supplemental Fig. S4D).

Collectively, the results of these experiments indicated that co-incubation of cancer cells with murine astrocytes, but not murine fibroblasts, leads to upregulation and activation of the endothelin signaling axis.

MDA-MB-231 Cancer Cell-derived IL-6 and IL-8 Upregulate Endothelin Signaling

Next, we reviewed the literature to identify potential upstream activators of the endothelin signaling axis. We focused on 2 inflammatory cytokines, IL-6 and IL-8, which are produced by cancer cells and have been shown to upregulate endothelin expression.[27,28] Co-incubation of MDA-MB-231 cells with astrocytes resulted in a 3-fold increase in IL-6 gene expression (Fig. 2A) and a 10-fold increase in IL-8 gene expression (Fig. 2B) in cancer cells. These results were confirmed by ELISA (Fig. 2C and D). The formation of gap junctions between astrocytes and MDA-MB-231 cells may be a prerequisite for IL-6 and IL-8 upregulation because both proteins were suppressed when we pre-incubated cancer cells with CBX. Moreover, we noted that the enhanced ET-1 production from astrocytes that were co-incubated with cancer cells declined to control levels when cancer cells were pretreated with CBX (Fig. 2E). The treatment of MDA-MB-231 cells with exogenous IL-6 or IL-8 significantly increased ET_AR and ET_BR expression on the cancer cells (Fig. 2F).

For confirmation, we transfected MDA-MB-231 cancer cells with siRNAs targeting IL-6 and IL-8 (Supplemental Figs S5A and S5B). Co-incubation of astrocytes with MDA-MB-231 cells transfected with siRNA targeting IL-6 for 24 hours decreased ET-1 gene expression by 30% in comparison to control cells or cells transfected with nontargeting control siRNA (Supplemental Fig. S5C), which was confirmed with ELISA (Supplemental Fig. S5D). Co-incubation of astrocytes with cancer cells transfected with siRNA targeting IL-8 reduced ET-1 gene expression by almost 75% compared with control or nontargeting siRNA, which was verified by ELISA. Similarly, stimulation of astrocytes with exogenous IL-6 or IL-8 significantly increased ET-1 gene expression (Supplemental Fig. S5E), and this was confirmed by ELISA (and S5F).

Collectively, these data demonstrated that gap junction signaling between astrocytes and MDA-MB-231 cells increases IL-6 and IL-8 production from cancer cells, which signal in an autocrine manner to upregulate ET receptor expression on cancer cells and in a paracrine manner to increase synthesis and secretion of ET-1 from astrocytes (Fig. 2G).

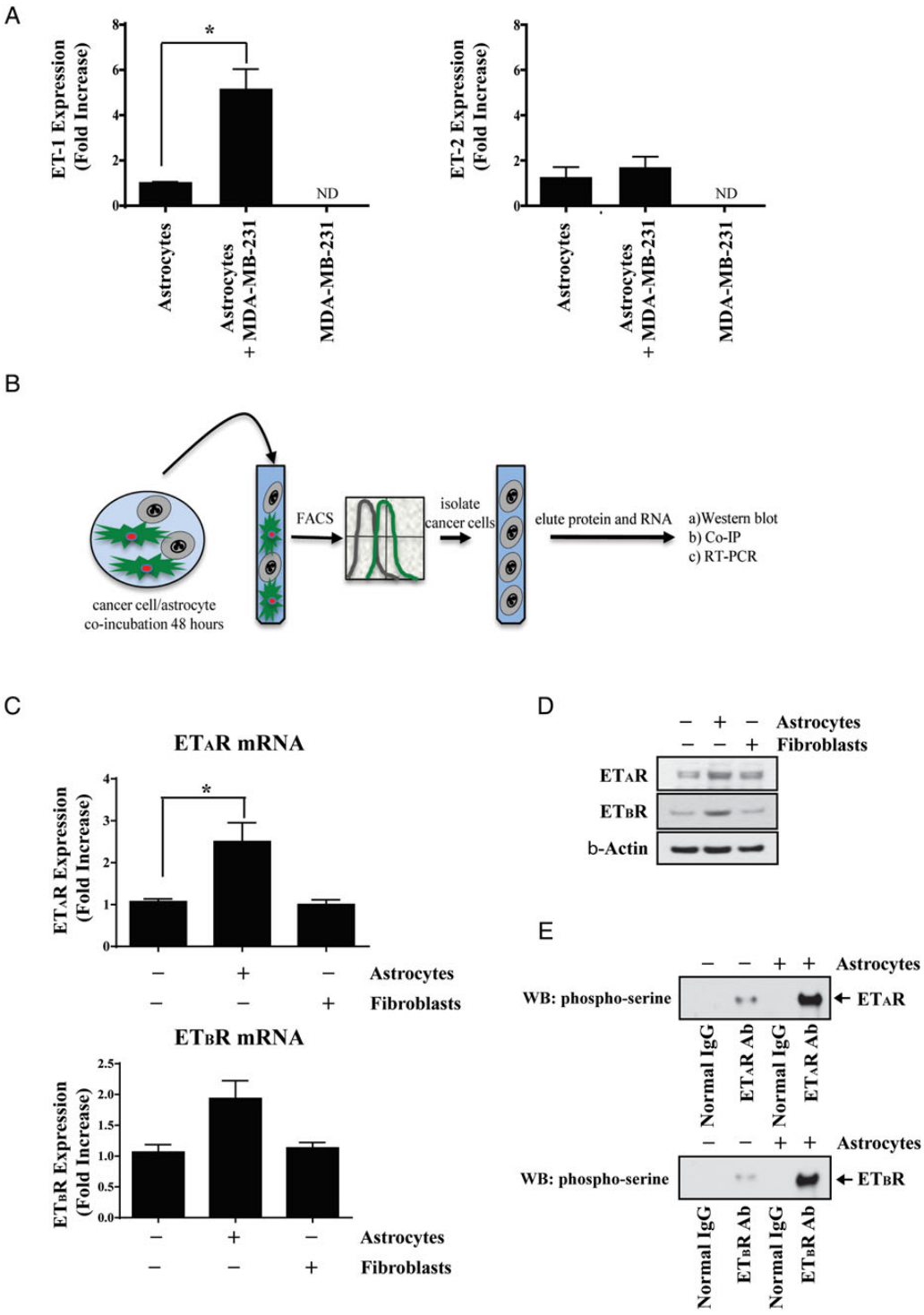

Fig. 1. Modulation of the endothelin axis in MDA-MB-231 cancer cells and astrocytes. (A) RT-PCR analysis of murine ET-1 expression in murine astrocytes, human MDA-MB-231 cancer cells and astrocytes, and MDA-MB-231 cancer cells that were co-incubated for 48 hours. (B) Schematic cartoon depicting the experimental approach used for parts C–E whereby GFP-labeled astrocytes or fibroblasts, which were co-incubated with human MDA-MB-231 cancer cells, were selectively removed so that analysis could be performed on cancer cells only. (C) RT-PCR analysis demonstrating that ET_AR and ET_BR are upregulated in MDA-MB-231 breast cancer cells cultured with GFP-labeled murine astrocytes, but not NIH 3T3 fibroblasts. (D) Western blot analysis of MDA-MB-231 cancer cells that were cultured alone or with astrocytes or fibroblasts. (E) Co-immunoprecipitation analysis demonstrating that ET_AR and ET_BR are phosphorylated on MDA-MB-231 cancer cells that were co-incubated with astrocytes but not fibroblasts. All figures are representative of 3 independent experiments. $^*P < .05$. ND, not detected.

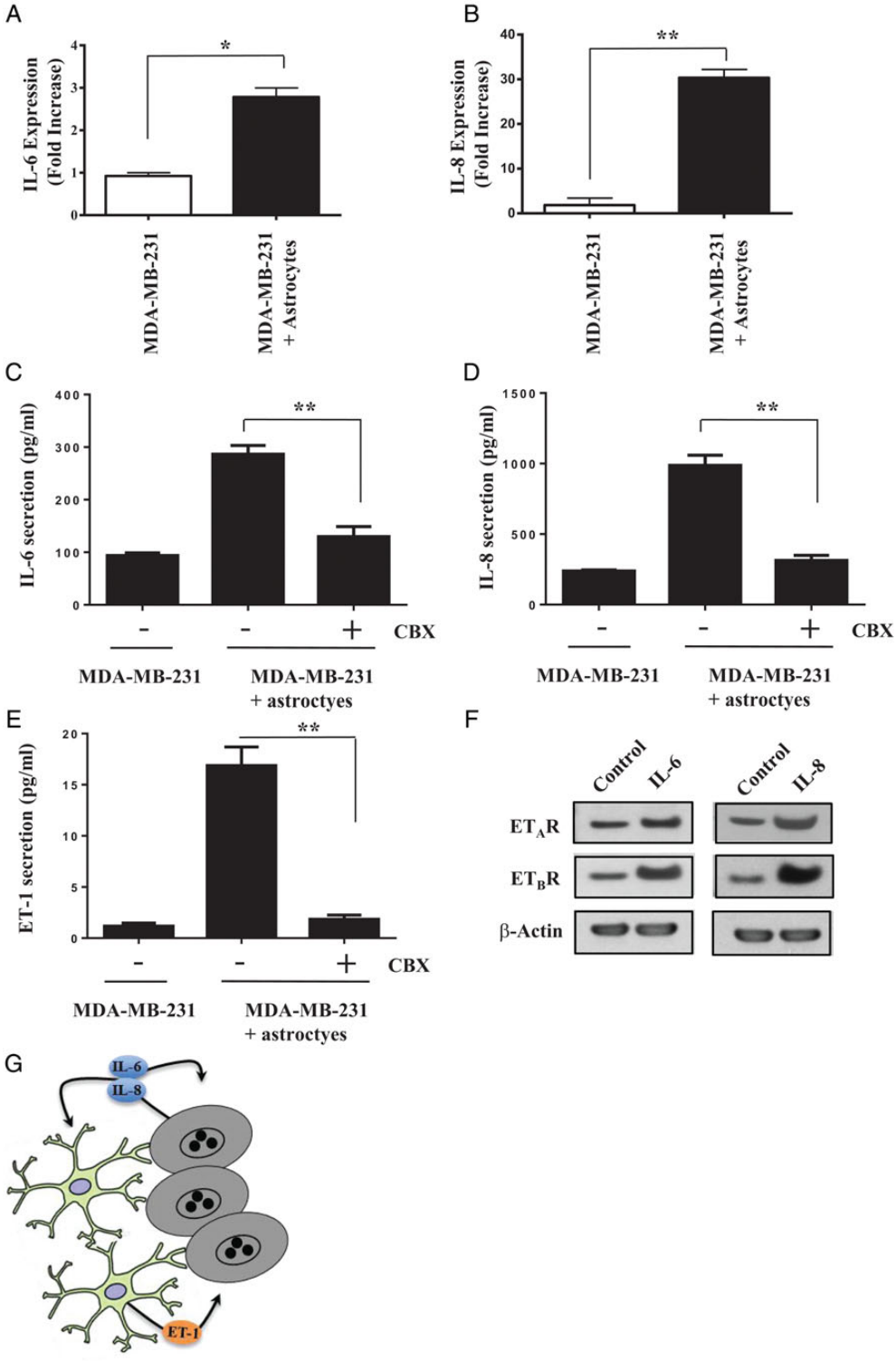

Fig. 2. MDA-MB-231 cancer cell-derived IL-6 and IL-8 upregulate endothelin signaling. (A) Co-incubation on astrocytes with cancer cells leads to upregulation of IL-6 and (B) IL-8 gene expression. (C) ELISA showing increased IL-6 and (D) IL-8 secretion when cancer cells are co-incubated for 24 hours with murine astrocytes. Treatment of MDA-MB-231 cells with 100 μM of the gap junction inhibitor CBX for 2 hours prior to co-incubation with astrocytes blocks IL-6 and IL-8 upregulation. (E) Treatment of MDA-MB-231 cancer cells with CBX for 2 hours prior to co-incubation with astrocytes blocks ET-1 secretion from astrocytes. (F) Western blot analysis of ET_AR and ET_BR expression in MDA-MB-231 cancer cells and cancer cells that were stimulated with 100 ng/mL of IL-6 or IL-8 proteins for 24 hours. (G) Cartoon depicting bidirectional signaling between murine astrocytes and MDA-MB-231 cancer cells (see text for details). $^*P < .05$, $^{**}P < .01$.

ET-1 Activates Endothelin Receptors, AKT and MAPK Signaling Pathways in MDA-MB-231 Cells

Because AKT/MAPK signaling pathways are upstream of genes associated with cell survival in cancer cells,[13] we evaluated the activation status of AKT and MAPK in MDA-MB-231 cells that were stimulated with ET-1. Stimulation of MDA-MB-231 cancer cells with 100 nM of ET-1 elicited robust phosphorylation of AKT and MAPK in a time-dependent manner (Fig. 3A). AKT and MAPK phosphorylation were detected as early as 5 minutes after treatment and peaked 2 hours later. Treatment with 50 nM of ET-1 resulted in phosphorylation of both AKT and MAPK within 5 minutes. We confirmed that ET-1-induced phosphorylation of AKT and MAPK by immunofluorescence microscopy (Fig. 3B). Treatment of the MDA-MB-231 breast cancer cells with 100 nM ET-1 resulted in phosphorylation of both ET_AR and ET_BR (Fig. 3C).

ET-1 Upregulates BCL2L1, GSTA5, and TWIST1 in MDA-MB-231 and H226 Cancer Cells

Previously, we reported that co-incubation of murine astrocytes with human breast cancer cells leads to the upregulation of cell survival genes in cancer cells that protect them from chemotherapy.[13] To determine if these effects are mediated by ET-1, we treated MDA-MB-231 cells with 100 nM of ET-1 once a day for 3 days and then measured *BCL2L1, GSTA5,* and *TWIST1* gene expression every 24 hours using RT-PCR. *TWIST1* expression increased by 6-fold in MDA-MB-231 cancer cells that were stimulated with ET-1 peptide for 72 hours when compared with untreated cells (Fig. 4A). *BCL2L1* and *GSTA5* gene expression levels increased by 4-fold and 3-fold, respectively, in MDA-MB-231 cancer cells that were stimulated with ET-1 for 72 hours. These results were validated using Western blot analysis (Fig. 4B).

To determine whether ET-1 upregulated *BCL2L1, GSTA5,* and *TWIST1* in other cancer cells, we stimulated H226 NSCLC cells with ET-1 and measured expression levels using RT-PCR. ET-1 increased *BCL2L1* expression by 9-fold in H226 cells after 72 hours of ET-1 stimulation (Fig. 4C). *GSTA5 and TWIST1* were also significantly increased in H226 cells after ET-1 stimulation, and these results were confirmed with Western blot analysis (Fig. 4D).

ET_AR and ET_BR Contribute to Astrocyte-induced Expression of Survival Genes in MDA-MB-231 Cancer Cells via the AKT/MAPK Signaling Pathway

Next, we wanted to determine which of the endothelin receptors was responsible (or if both were responsible) for astrocyte-induced activation of AKT/MAPK signaling in cancer cells. We pre-incubated MDA-MB-231 cancer cells with the ET_AR antagonist (BQ123), ET_BR antagonist (BQ788), both ET_AR and ET_BR antagonists (BQ123 plus BQ788), or the dual endothelin receptor antagonist, macitentan. MDA-MB-231 cancer cells were cultured alone or with GFP-labeled murine astrocytes for 6 hours, and then the cancer cells were collected by cell sorting with FACS analysis and prepared for Western blot analysis. The phosphorylated forms of AKT and MAPK were markedly increased in cancer cells that were incubated with astrocytes in comparison with cancer cells that were growing alone (Fig. 5A). Single-agent treatment with either BQ123 or BQ788 had little effect on AKT and MAPK phosphorylation in MDA-MB-231 cancer cells that were co-incubated with astrocytes. In contrast, astrocyte-induced AKT and MAPK phosphorylation were significantly attenuated by combination treatment with BQ123 and BQ788 or by macitentan alone.

Next, we examined the effects of the various ET_AR and ET_BR antagonists on *BCL2L1, GSTA5*, and *TWIST1* gene expression. MDA-MB-231 breast cancer cells were pre-incubated with endothelin receptor antagonists, co-incubated with GFP-labeled astrocytes for 24 hours, and then isolated from astrocytes using FACS analysis. Single-agent treatment with BQ123 or BQ788 had no effect on astrocyte-induced upregulation of *BCL2L1, GSTA5*, and *TWIST1* (Fig. 5B). However, combined treatment with both BQ123 and BQ788 or macitentan alone completely abrogated astrocyte-induced upregulation of survival genes in the cancer cells. These results were confirmed by Western blot (Fig. 5C) and demonstrated that combined inhibition of both ET_AR and ET_BR signaling pathways is required to block AKT/MAPK activation and the resulting survival gene expression in MDA-MB-231 cells.

Both ET_AR and ET_BR Contribute to Astrocyte-mediated Protection of Cancer Cells from Chemotherapeutic Agents

We then investigated the role of endothelin receptors on astrocyte-mediated protection of cancer cells from taxol by using ET_AR and ET_BR siRNAs. Specific downregulation of corresponding protein expression by siRNA was confirmed by Western blot analysis (Fig. 6A). Next, we compared the apoptotic index of MDA-MB-231 cells and the transfected cancer cells that were cultured alone in the presence of 15 ng/mL taxol with that of cancer cells that were co-incubated with murine astrocytes in taxol. The apoptotic index of the cancer cells incubated with murine astrocytes was significantly reduced in comparison with cancer cells that were cultured alone (48.4 ± 4.8 vs 34.1 ± 3.4; $P < .05$) (Fig. 6B). The protective effect was still observed in cancer cells transfected with nontargeting siRNA (48.9 ± 3.4 vs 28.5 ± 7.4; $P < .05$), siRNA targeting only ET_AR (53.5 ± 3.8 vs 29.3 ± 4.1; $P < .05$), and siRNA targeting only ET_BR (53.4 ± 6.3 vs 29.4 ± 7.6; $P < .05$). However, protection from chemotherapy was abolished in MDA-MB-231 cancer cells that were transfected with siRNAs targeting both ET_AR and ET_BR (46.2 ± 3.6 vs 44.7 ± 2.5; $P = .69$).

Next, we conducted an assay employing type-specific ET_AR and ET_BR antagonists to confirm that dual inhibition of these receptors is critical for abolishing astrocyte-mediated protection from chemotherapeutic agents. MDA-MB-231 cancer cells were pre-incubated with BQ123, BQ788, both antagonists, or macitentan and were then cultured for 48 hours in the presence of taxol with or without GFP-labeled murine astrocytes. Cancer cells cultured with astrocytes had a significantly reduced apoptotic index when compared with cancer cells that were cultured alone (42.1 ± 1.3 vs 25.5 ± 3.1; $P < .05$) (Fig. 6C). The single endothelin antagonists BQ123 (41.3 ± 2.6 vs 26.3 ± 3.7; $P < .05$) and BQ788 (43.8 ± 2.0 vs 32.3 ± 2.7; $P < .05$) had no effect on astrocyte-mediated chemoprotection. In contrast, protection from chemotherapy was eliminated in cancer cells that were treated with the combination of BQ123 and BQ788 (42.1 ± 1.4 vs 40.3 ± 2.8; $P = .31$) or with macitentan alone (45.8 ± 3.2 vs 42.2 ± 6.1; $P = .42$). The co-incubation of astrocytes with cancer cells had negligible effect on the cell cycle profile of MDA-MB-231 cells: MDA-MB-231 cells cultured alone (G1 45%; S 25%; G2/M 30%) versus MDA-MB-231 co-cultured with astrocytes (G1 44%; S 24%; G2/M 32%).

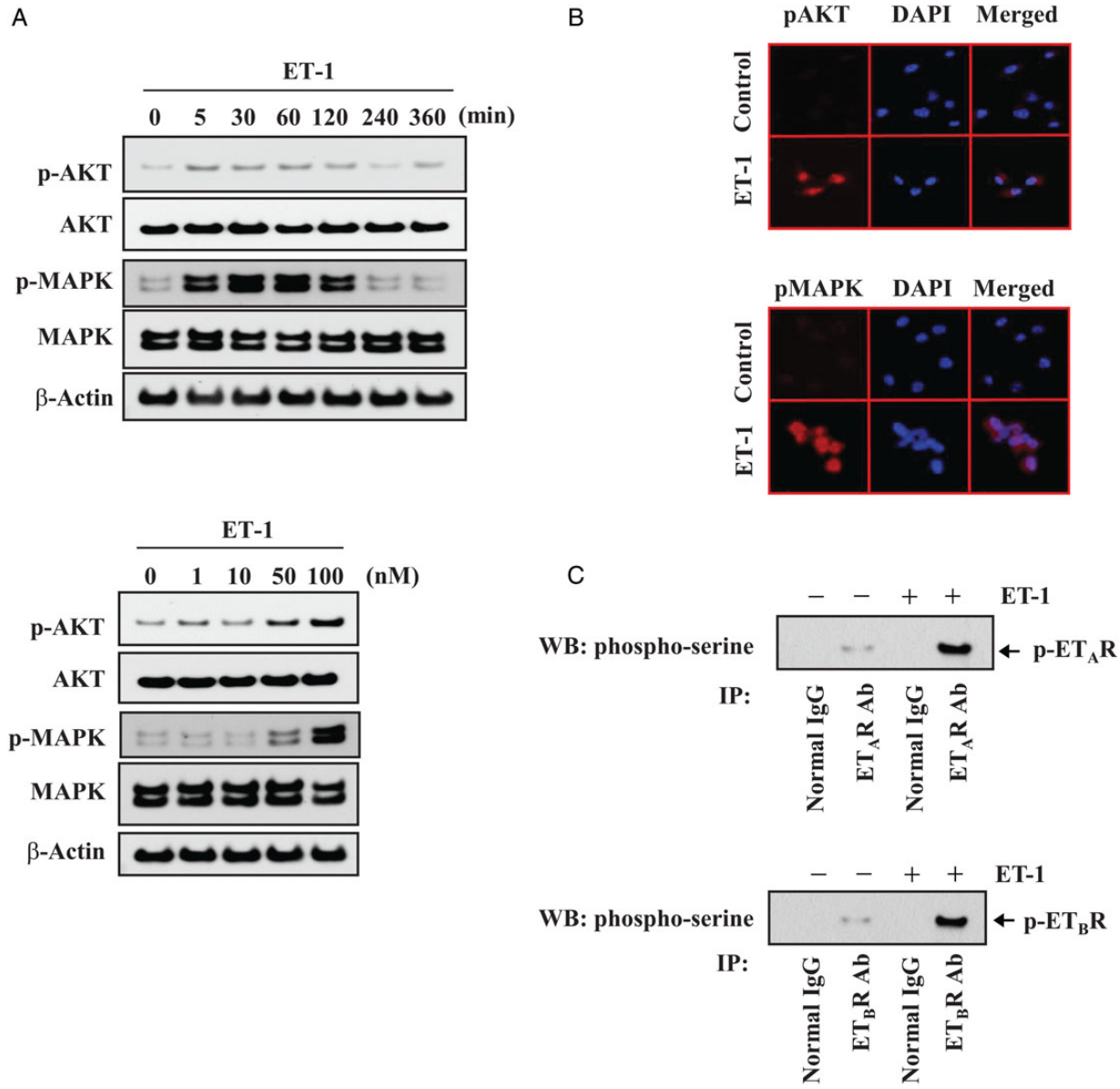

Fig. 3. ET-1 phosphorylates AKT/MAPK signaling pathways in MDA-MB-231 cancer cells. (A) Western blot analysis of total and activated forms of AKT and MAPK in MDA-MB-231 cancer cells incubated with 100 nM ET-1 for the indicated periods (upper panel) or with ET-1 at the indicated concentrations for 30 minutes (lower panel). (B) Immunofluorescence staining of phospho-AKT (upper panel) and phospho-MAPK (bottom panel). Cells were incubated for 30 minutes with vehicle or 100 nM ET-1 and then labeled with antibodies directed against the phosphorylated forms of AKT and MAPK (red). Nuclei were stained with DAPI (blue). (C) MDA-MB-231 cancer cells were incubated for 30 minutes with 100 nM ET-1. Cell lysates were subjected to immunoprecipitation and Western blotting, as described in Figure 2. Control immunoprecipitations were performed with normal mouse or rabbit IgG.

We confirmed the chemoprotection results of mouse astrocytes with human astrocytes. MDA-MB-231 cells co-incubated with human astrocytes and MDA-MB-231 cells that were transfected with nontargeting siRNA, siRNA targeting only ET_AR, and siRNA targeting only ET_BR were protected from taxol when compared with cancer cells alone ($P < .01$) (Fig. 6D). The human astrocyte-induced chemoprotective effect was abrogated in cells with siRNAs targeting both ET_AR and ET_BR (66.93 ± 7.9 vs 57.4 ± 2.0; $P < .05$). None of the transfections had an impact on the apoptotic index in the absence of taxol. We also found that the apoptotic index of cancer cells incubated with human astrocytes was significantly reduced when compared with MDA-MB-231 cancer cells growing alone (Fig. 6E) (43.3 ± 2.6 vs 26.1 ± 3.6; $P < .05$). Neither BQ123 (43.2 ± 6.0 vs 27.8 ± 1.9; $P < .05$) nor BQ788 (43.8 ± 3.8 vs 26.0 ± 4.2; $P < .05$) prevented the astrocyte-mediated chemoprotection effect. In contrast, protection from chemotherapy was lost in tumor cells pretreated with both endothelin receptor antagonists (46.6 ± 8.4 vs 42.5 ± 7.2; $P = .01$) or with macitentan (50.6 ± 2.3 vs 41.1 ± 2.8; $P = .01$).

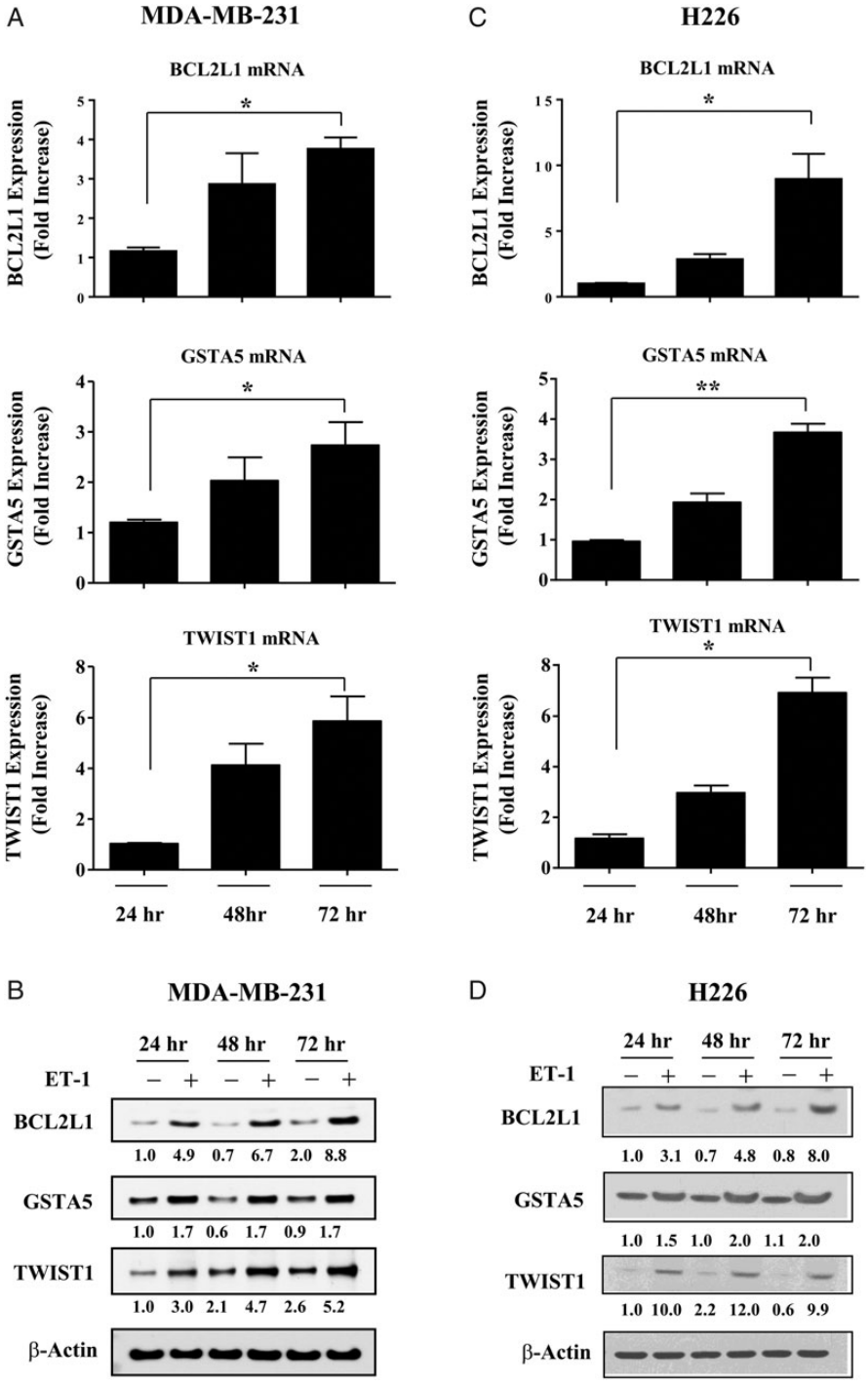

Fig. 4. ET-1 increases gene expression of *BCL2L1*, *GSTA5*, and *TWIST1* in cancer cells. (A) MDA-MB-231 cancer cells were stimulated with 100 nM ET-1, and gene expression levels of *BCL2L1*, *GSTA5*, and *TWIST1* were measured every 24 hours with RT-PCR. Fold increase refers to the ratio of mRNA levels in ET-1 treated cells to that of 24-hour treated cells. (B) Western blot analysis comparing protein expression of $Bcl2_l1$, Gsta5, and Twist1 in untreated MDA-MB-231 cancer cells with cells that were stimulated with 100 nM ET-1. (C) H226 NSCLC cells were stimulated with 100 nM ET-1, and gene expression levels of *BCL2L1*, *GSTA5*, and *TWIST1* were measured every 24 hours with RT-PCR. (D) Western blot analysis comparing protein expression of $Bcl2_l1$, Gsta5, and Twist1 in untreated H226 NSCLC cells with cells that were stimulated with 100 nM ET-1. Protein levels were quantified by densitometry using ImageJ 1.40 software. ß-Actin expression was used as an internal control. Statistical significances are compared with 24-hour treated cells. $^{*}P < .05$, $^{**}P < .01$.

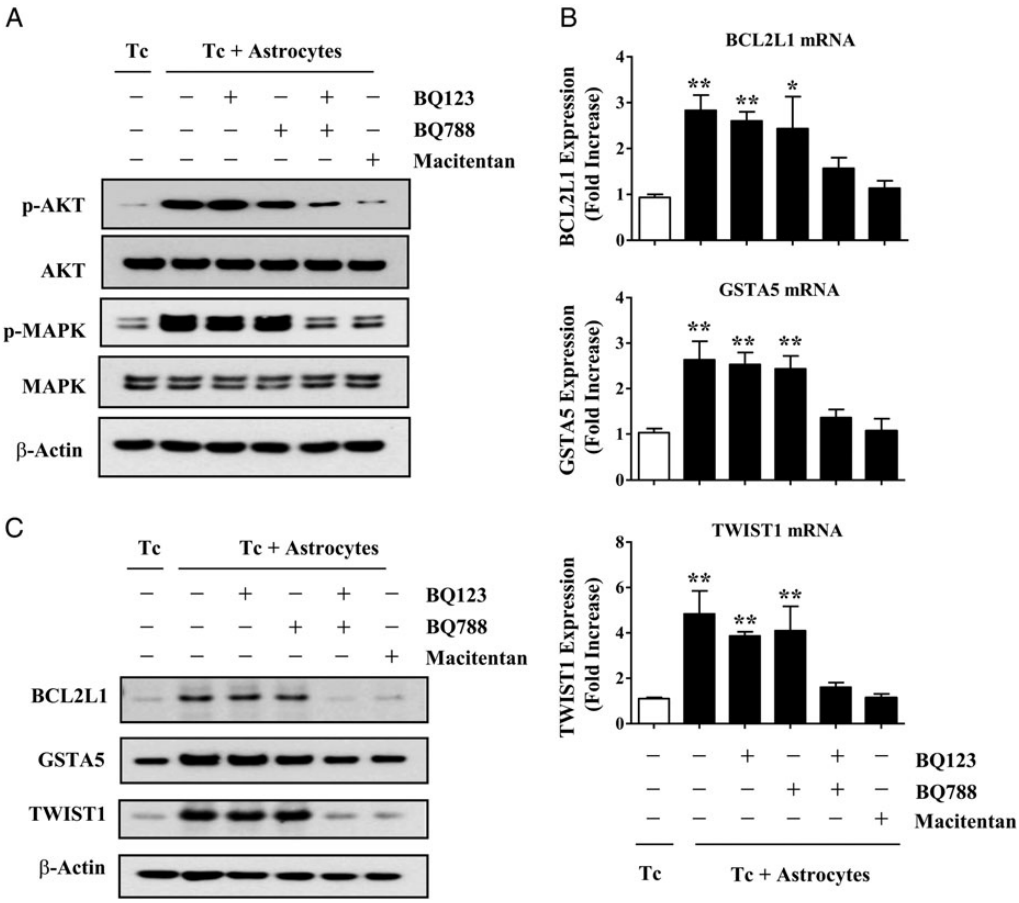

Fig. 5. Dual antagonism of ET_AR and ET_BR block astrocyte-induced activation of AKT/MAPK signaling and anti-apoptotic gene expression in MDA-MB-231 cancer cells. (A) Western blot analysis of MDA-MB-231 cancer cells that were pre-incubated for 2 hours with 1 μM BQ123, 1 μM BQ788, BQ123 plus BQ788, or 100 nM macitentan and then cultured alone (Tc) or co-incubated with murine astrocytes (Tc + astrocytes). GFP-labeled astrocytes were removed by FACS, and Western blot was performed on cancer cells as described in Material and Methods. (B) RT-PCR analysis of *BCL2L1*, *GSTA5*, and *TWIST1* expression in MDA-MB-231 cancer cells cultured alone or co-incubated with murine astrocytes. Target gene expression levels were normalized to the 18S rRNA level. Fold increase refers to the ratio of mRNA levels in MDA-MB-231 cells cultured alone versus cells co-incubated with GFP-labeled murine astrocytes. (C) Western blot analysis of Bcl2$_l$1, Gsta5, and Twist1expressed by MDA-MB-231 cancer cells alone or cells that were co-incubated with astrocytes for 48 hours. ß-Actin expression was used as an internal control for Western blotting. Values shown are means ± SD of 3 independent experiments, each performed with triplicate cultures. Statistical significances were compared with cancer cell growing alone. $^*P < .05$, $^{**}P < .01$.

Collectively, these results suggested that both murine astrocytes and human astrocytes mediate the protection of cancer cells from taxol through ET_AR and ET_BR signaling pathways. Only simultaneous knockdown or dual antagonism of these receptors abolished astrocyte-mediated chemoprotection of cancer cells.

Astrocyte-induced Upregulation of Survival Proteins in Cancer Cells Is Dependent on Gap Junction-mediated Communication

The initiating signal between astrocytes and cancer cells was dependent on gap junction communication. To determine if ensuing upregulation of anti-apoptotic proteins was due to a soluble astrocyte factor, we stimulated MDA-MB-231 cancer cells in astrocyte-conditioned media for 48 hours and measured *BCL2L1, GSTA5*, and *TWIST1* gene expression levels (Supplementary Fig. S6A). Astrocyte-conditioned media had no effect on anti-apoptotic gene expression, and this was confirmed by Western blot analysis (Supplementary Fig. S6B). The expression of anti-apoptotic proteins also remained unchanged when MDA-MB-231 cancer cells were separated from astrocytes by a 0.4-μm pore membrane (Supplementary Fig. S6C). However, pretreatment of cancer cells with the gap junction channel inhibitor CBX abolished astrocyte-induced chemoprotection (Supplementary Fig. 6D). These data suggested that astrocyte-induced upregulation of anti-apoptotic proteins and chemoprotection of cancer cells are dependent on coupling of astrocytes and cancer cells through gap junction channels.

Brain-derived Endothelial Cells, But Not Microglial Cells, Protect Cancer Cells from Chemotherapy

Next, we questioned whether other CNS cells might also protect cancer cells from chemotherapy. We found that murine brain

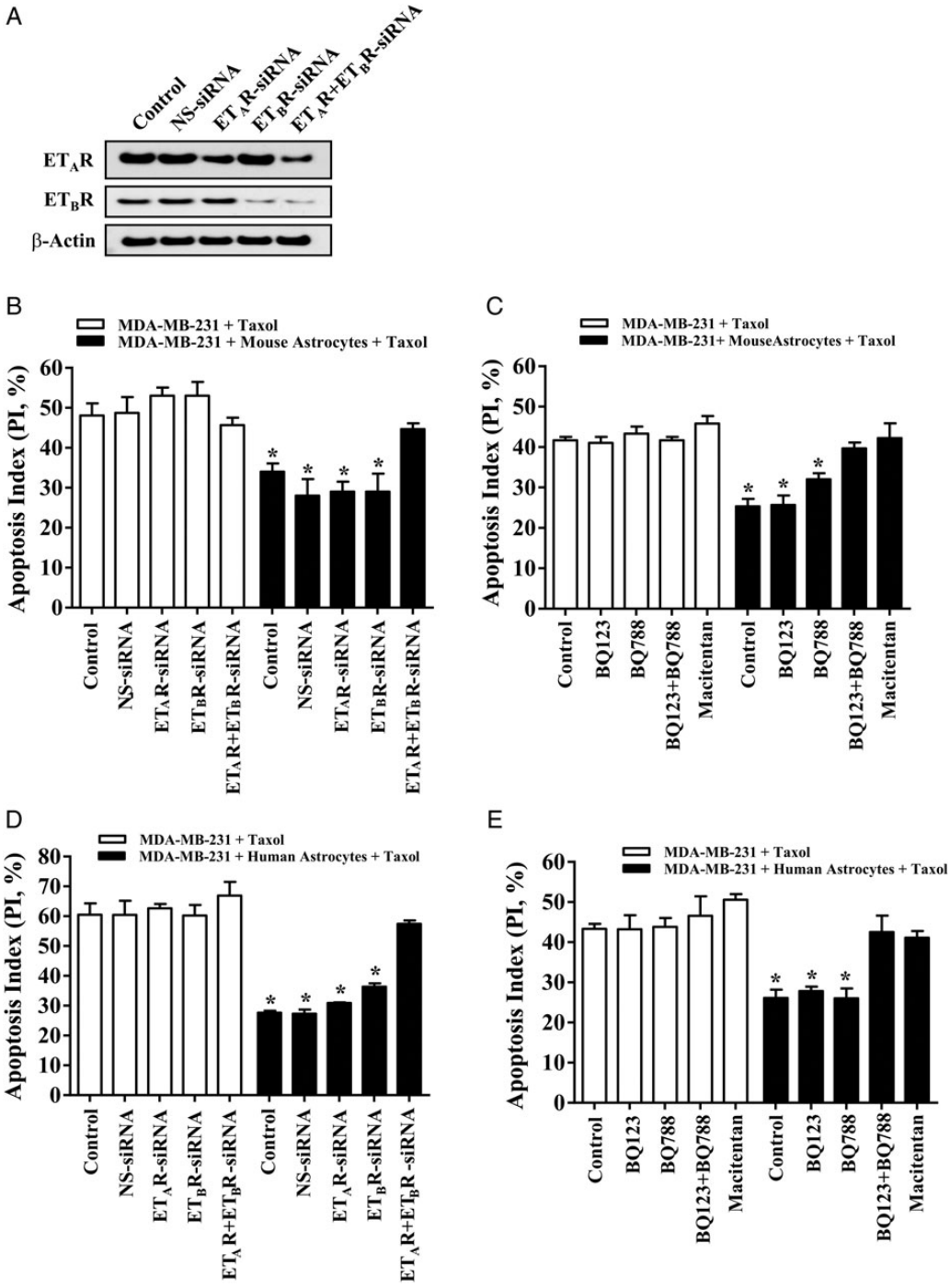

Fig. 6. Activation of both ET_AR and ET_BR is essential for astrocyte-mediated chemoprotection of cancer cells. (A) MDA-MB-231 cancer cells were transfected with 100 nM siRNA targeting ET_AR (ET_AR-siRNA), ET_BR (ET_BR-siRNA), or both ($ET_AR + ET_BR$ siRNA). Nonspecific control siRNA (NS-siRNA) was used as a control. (B) Comparison of the apoptotic index of MDA-MB-231 cancer cells and siRNA transfected MDA-MB-231 cancer cells cultured alone in the presence of taxol with cancer cells co-incubated with murine astrocytes in the presence of taxol. (C) Chemoprotection assay in which MDA-MB-231 cancer cells were pre-incubated for 2 hours with 1 μM of BQ123, BQ788, both antagonists, or the dual antagonist, macitentan (100 nM) and then cultured alone (control) or co-incubated with GFP-labeled murine astrocytes in the presence of taxol (15 ng/mL). (D) Chemoprotection assay with siRNA transfected MDA-MB-231 cancer cells and human astrocytes. (E) Chemoprotection assay with MDA-MB-231 cells treated with endothelin antagonists and co-incubated with human astrocytes. $^*P < .05$ versus control cancer cells growing alone in the presence of taxol.

endothelial cells[24] protected MDA-MB-231 cancer cells from taxol and that this protection was dependent on gap junction communication between the 2 cell types (Supplementary Fig. S7A). We confirmed the role of endothelin signaling in brain endothelial cell-mediated chemoprotection by using the ET_AR and ET_BR siRNA-transfected cancer cells. The apoptotic index of MDA-MD-231 cells that were co-incubated with brain endothelial cells treated with taxol was 50% of cancer cells alone in taxol. Only siRNA targeting of both endothelin receptors eliminated the chemoprotective effect of brain endothelial cells (Supplementary Fig. S7B). Microglial cells had no effect on the responsiveness of cancer cells to chemotherapy (Supplementary Fig. S7C).

Finally, to verify gap junction communication between MDA-MB-231 cancer cells and brain endothelial cells (and cancer cells and astrocytes) we used a FACS-based dye transfer assay. Donor brain endothelial cells and astrocytes were labeled with calcein and then co-incubated with DiI-labeled cancer cells (recipient cells). After a 6 hour co-incubation period, we noted that cancer cells formed gap junction communication with donor astrocytes and endothelial cells as evidenced by the transfer of calcein from donor cells to cancer cells (Supplementary Figs S8A and S8B). Pretreatment of MDA-MB-231 cancer cells with CBX reduced the number of calcein-containing cancer cells. No calcein was transferred to cancer cells when they were separated from donor astrocytes and endothelial cells in transwell chambers (data not shown).

Discussion

Most reports seeking to explain the inability of systemic therapy to improve clinical outcomes for patients with brain metastases have invoked a role for the blood-brain barrier and efflux transporters such as P-glycoprotein.[5,6,8] Until recently, virtually no information was available regarding the role of astrocytes in mediating therapeutic resistance. We have previously reported that astrocytes protect cancer cells from chemotherapy by stimulating the upregulation of a subset of anti-apoptotic genes in cancer cells.[13] Here, we demonstrated that astrocyte-induced survival gene expression in MDA-MB-231 breast cancer cells and H226 NSCLC cells and the ensuing protection of the cancer cells from chemotherapy are products of an upregulated and activated endothelin signaling axis. We also showed, for the first time, that brain endothelial cells protect cancer cells from chemotherapy by an endothelin-dependent mechanism. Therapeutic antagonists of either ET_AR or ET_BR on MDA-MB-231 breast cancer cells have little effect on astrocyte-mediated chemoprotection, whereas simultaneous antagonism of both endothelin receptors prevents activation of intracellular AKT and MAPK effector proteins that are responsible for expression of survival genes, thus rendering cancer cells responsive to chemotherapy.

Accumulating evidence suggests that upregulation of endothelin peptides is a characteristic feature of the reactive astrogliosis that accompanies CNS pathologies[17] including brain metastasis.[16] We found that co-incubation of MDA-MB-231 cancer cells and H226 cancer cells with astrocytes led to upregulated expression of ET-1 by astrocytes and significantly enhanced ET_AR and ET_BR expression on the cancer cells. The current study builds on our previous efforts in that we define a critical role for cancer cell-derived IL-6 and IL-8 in upregulating the endothelin axis. Indeed, this finding underscores the complexity of the cell-cell interactions that take place in the tumor microenvironment. However, not all cell types are endowed with chemoprotective potential; fibroblasts and microglial cells failed to protect cancer cells from taxol. The finding that astrocytes function as the endothelin-releasing cell is consistent with results generated from clinical studies of brain metastases demonstrating that peritumoral astrocytes overexpress endothelin in 85% of cases.[15] Similarly, the finding that brain endothelial cells protect cancer cells from chemotherapy through an endothelin-dependent mechanism is reasonable, given that endothelial cells are the primary cellular source of endothelin in the body.[14]

The administration of exogenous ET-1 to cancer cells or co-incubation of cancer cells with astrocytes elicits a rapid, robust increase in the expression of the phosphorylated forms of AKT and MAPK. AKT and MAPK proteins play an important regulatory role in a number of diverse cellular processes including cell survival.[29] Results generated from other laboratories have shown that activation of AKT and MAPK signaling pathways leads to upregulation of the anti-apoptotic genes encoding *BCL2L1*,[29] *GSTA5*,[30] and *TWIST1*.[31] In the present report, we noted that stimulation of MDA-MB-231 cancer cells with exogenous ET-1 peptides or co-incubation of the cancer cells with astrocytes resulted in marked upregulation of *BCL2L1*, *GSTA5*, and *TWIST1*. Consequently, overexpression of these genes decreases apoptosis and improves cell survival. Moreover, we previously reported that inhibition of these 3 proteins abolishes protection from chemotherapy.[13]

Similar to our previous report demonstrating that astrocyte-induced chemoprotection of melanoma cells requires direct physical contact between the 2 cell types,[12] astrocyte- and brain endothelial cell-mediated protection of breast cancer cells and lung cancer cells from taxol was also dependent on formation of gap junctions. The melanoma study invoked a role for connexin 43 expressed on the cell surface of melanoma cells and astrocytes in promoting resistance to chemotherapy, inasmuch as silencing connexin 43 eliminated astrocyte-induced protection. Currently, there are 21 connexin isoforms in the human proteome with different physiological properties and regulatory responses.[32] It will be important to determine which connexin subunits are involved in breast and lung cancer chemoprotection and how the ensuing IL-6 and IL-8 signaling between cancer cells and astrocytes transpires (eg, direct shuttling vs exosomes, etc.).

The advent of endothelin antagonists has also resulted in a deeper appreciation of the complexity of endothelin signaling that takes place during tumor progression and metastasis. For example, it is now known that prostate cancer cell–produced ET-1 stimulates new bone formation in vitro and osteoblastic metastases in vivo by signaling through the ET_AR expressed on osteoblasts.[33] Similarly, more recent experimental studies determined that bladder cancer cell–derived ET-1 signals for recruitment of a population of ET_AR^+ macrophages to the lung, which then creates a prometastatic inflammatory microenvironment that is conducive for metastatic growth.[34] Similar to these reports, our results suggest an important role for paracrine ET-1 signaling between cancer cells and stromal cells as a mechanism that sustains cancer cell viability. To our knowledge, the present study is the first to demonstrate that communication between astrocytes and cancer cells involves upregulation and activation of the endothelin axis.

Identifying the cellular and molecular mechanisms that mediate therapeutic resistance of cancer cells in the brain has been challenging. The clinical problem is emphasized by a recent study on newly diagnosed, previously untreated patients with small cell lung cancer brain metastases who had an intracranial response rate of 27% and an extracranial response rate of 73%.[35] While the blood-brain barrier plays a role in limiting the uptake of chemotherapeutic agents into the brain parenchyma and much recent effort has been directed toward identifying agents with improved penetrating properties, the results to date from studies evaluating agents such as temozolamide have been disappointing.[3,36,37] The results of the present study suggest that therapeutic targeting of astrocyte- and endothelial cell-mediated protection of cancer cells from chemotherapy by antagonism of endothelin receptor signaling may represent a novel approach for improving the efficacy of treatments for brain metastasis.

Supplementary Material

Supplementary material is available online at Neuro-Oncology (http://neuro-oncology.oxfordjournals.org/).

Funding

This work was supported in part by Cancer Center Support Core grant CA16672, grant 2RO1-CA154710 from the National Cancer Institute, National Institutes of Health, and by sponsored research from Actelion Pharmaceuticals, Ltd.

Conflict of interest statement. None declared.

References

1. Gavrilovic IT, Posner JB. Brain metastases: epidemiology and pathophysiology. *J Neurooncol*. 2005;75(1):5–14.
2. Cruz-Munoz W, Kerbel RS. Preclinical approaches to study the biology and treatment of brain metastases. *Semin Cancer Biol*. 2011;21(2):123–130.
3. Kienast Y, Winkler F. Therapy and prophylaxis of brain metastases. *Expert Rev Anticancer Ther*. 2010;10(11):1763–1777.
4. Walbert T, Gilbert MR. The role of chemotherapy in the treatment of patients with brain metastases from solid tumors. *Int J Clin Oncol*. 2009;14(4):299–306.
5. Deeken JF, Loscher W. The blood-brain barrier and cancer: transporters, treatment, and Trojan horses. *Clin Cancer Res*. 2007;13(6):1663–1674.
6. Loscher W, Potschka H. Drug resistance in brain diseases and the role of drug efflux transporters. *Nat Rev Neurosci*. 2005;6(8):591–602.
7. Zhang RD, Price JE, Fujimaki T, et al. Differential permeability of the blood-brain barrier in experimental brain metastases produced by human neoplasms implanted into nude mice. *Am J Pathol*. 1992;141(5):1115–1124.
8. Lockman PR, Mittapalli RK, Taskar KS, et al. Heterogeneous blood-tumor barrier permeability determines drug efficacy in experimental brain metastases of breast cancer. *Clin Cancer Res*. 2010;16(23):5664–5678.
9. Frosch MP, Anthony DC, De Girolami U. The Central Nervous System. In: Kumar V, Abbas AK, Fausto N, Aster JC, eds. *Robbins and Cotran Pathologic Basis of Disease*. 8th ed. Philadelphia, PA: Saunders Elsevier; 2010:1279–1344.
10. Fitzgerald DP, Palmieri D, Hua E, et al. Reactive glia are recruited by highly proliferative brain metastases of breast cancer and promote tumor cell colonization. *Clin Exp Metastasis*. 2008;25(7):799–810.
11. Lorger M, Felding-Habermann B. Capturing changes in the brain microenvironment during initial steps of breast cancer brain metastasis. *Am J Pathol*. 2010;176(6):2958–2971.
12. Lin Q, Balasubramanian K, Fan D, et al. Reactive astrocytes protect melanoma cells from chemotherapy by sequestering intracellular calcium through gap junction communication channels. *Neoplasia*. 2010;12(9):748–754.
13. Kim SJ, Kim JS, Park ES, et al. Astrocytes upregulate survival genes in tumor cells and induce protection from chemotherapy. *Neoplasia*. 2011;13(3):286–298.
14. Kedzierski RM, Yanagisawa M. Endothelin system: the double-edged sword in health and disease. *Annu Rev Pharmacol Toxicol*. 2001;41:851–876.
15. Zhang M, Olsson Y. Reactions of astrocytes and microglial cells around hematogenous metastases of the human brain. Expression of endothelin-like immunoreactivity in reactive astrocytes and activation of microglial cells. *J Neurol Sci*. 1995;134:26–32.
16. Nie XJ, Olsson Y. Endothelin peptides in brain diseases. *Rev Neurosci*. 1996;7(3):177–186.
17. Cruz-Munoz W, Jaramillo ML, Man S, et al. Roles for endothelin receptor B and BCL2A1 in spontaneous CNS metastasis of melanoma. *Cancer Res*. 2012;72(19):4909–4919.
18. Egidy G, Eberl LP, Valdenaire O, et al. The endothelin system in human glioblastoma. *Lab Invest*. 2000;80(11):1681–1689.
19. Del Bufalo D, Di Castro V, Biroccio A, et al. Endothelin-1 protects ovarian carcinoma cells against paclitaxel-induced apoptosis: requirement for Akt activation. *Mol Pharmacol*. 2002;61(3):524–532.
20. Rosano L, Spinella F, Bagnato A. Endothelin 1 in cancer: biological implications and therapeutic opportunities. *Nat Rev Cancer*. 2013;13(9):637–651.
21. Iglarz M, Binkert C, Morrison K, et al. Pharmacology of macitentan, an orally active tissue-targeting dual endothelin receptor antagonist. *J Pharmacol Exp Ther*. 2008;327(3):736–745.
22. Yano S, Shinohara H, Herbst RS, et al. Expression of vascular endothelial cell growth factor is necessary but not sufficient for prodcution and growth of brain metastases. *Cancer Res*. 2000;60(17):4959–4967.
23. Langley RR, Fan D, Guo L, et al. Generation of an immortalized astrocyte cell line from H-2Kb-tsA58 mice to study the role of astrocytes in brain metastasis. *Int J Oncol*. 2009;35(4):665–672.
24. Langley RR, Ramirez KM, Tsan RZ, et al. Tissue-specific microvascular endothelial cell lines from H-2 K(b)-tsA58 mice for studies of angiogenesis and metastasis. *Cancer Res*. 2003;63(11):2971–2976.
25. Dull T, Zufferey R, Kelly M, et al. A third-generation lentivirus vector with a conditional packaging system. *J Virol*. 1998;72(11):8463–8471.
26. Livak KJ, Schmittgen TD. Analysis of relative gene expression data using real-time quantitative PCR and the 2(-Delta Delta C(T)) Method. *Methods*. 2001;25(4):402–408.
27. Yamashita J, Ogawa M, Nomura, et al. Interleukin 6 stimulates the production of immunoreactive endothelin 1 in human breast cancer cells. *Cancer Res*. 1993;53(3):464–467.
28. Endo T, Uchida Y, Matsumoto H, et al. Regulation of endothelin-1 synthesis in cultured guinea pig airway epithelial cells by

various cytokines. *Biochem Biophys Res Commun*. 1992;186(3): 1594–1599.

29. Yu YL, Chiang YJ, Chen YC, et al. MAPK-mediated phosphorylation of GATA-1 promotes Bcl-XL expression and cell survival. *J Biol Chem*. 2005;280(33):29533–29542.
30. Kazi S, Ellis EM. Expression of rat liver glutathione-S-transferase GSTA5 in cell lines provides increased resistance to alkylating agents and toxic aldehydes. *Chem Biol Interact*. 2002;140(2): 121–135.
31. Zhang X, Wang Q, Ling MT, et al. Anti-apoptotic role of TWIST and its association with Akt pathway in mediating taxol resistance in nasopharyngeal carcinoma cells. *Int J Cancer*. 2007;120(9): 1891–1898.
32. Maeda S, Tsukihara T. Structure of the gap junction channel and its implications for its biological functions. *Cell Mol Life Sci*. 2011;68(7): 1115–1129.
33. Yin JJ, Mohammad KS, Kakonen SM, et al. A causal role for endothelin-1 in the pathogenesis of osteoblastic bone metastases. *Proc Natl Acad Sci USA*. 2003;100(19):10954–10959.
34. Said N, Smith S, Sanchez-Carbayo M, et al. Tumor endothelin-1 enhances metastatic colonization of the lung in mouse xenograft models of bladder cancer. *J Clin Invest*. 2011;121(1):132–147.
35. Seute T, Leffers P, Wilmink JT, et al. Response of asymptomatic brain metastases from small-cell lung cancer to systemic first-line chemotherapy. *J Clin Oncol*. 2006;24(13):2079–2083.
36. Eichler AF, Chung E, Kodack DP, et al. The biology of brain metastases-translation to new therapies. *Nat Rev Clin Oncol*. 2011; 8(6):344–356.
37. Platta CS, Khuntia D, Mehta MP, et al. Current treatment strategies for brain metastasis and complications from therapeutic techniques: a review of current literature. *Am J Clin Oncol*. 2010; 33(4):398–407.